Analytical expressions of unsteady ship wave patterns

X.B. CHEN & L. DIEBOLD

Bureau Veritas, DTA, 17bis, Place des Reflets, 92400 Courbevoie (FRANCE)
Fax: 33-1-4291.3395 Email: xchen@bureauveritas.com

The time-harmonic ship wave patterns are studied by considering free-surface potential flows generated by a point source pulsating and advancing at a uniform forward speed. New expressions in analytically closed form are obtained by an asymptotic analysis on the wave component which is represented by a single Fourier integral along the dispersion curves defined in the Fourier plane by the dispersion relation. These new expressions together with the results given in [1] including simple relations between the dispersion curves and important aspects (wavelengths, directions of wave propagation, phase and group velocities, and cusp angles) of the corresponding far-field waves, draw a complete and analytical picture of unsteady ship wave patterns.

1 Generic representation of wave components

Within an analysis in frequency domain, the time-harmonic velocity potential $\mathcal{G}(\vec{\xi})$ at a field point $\vec{\xi}=(\xi,\eta,\zeta)$ can be expressed in the form $\mathcal{G}^S+\mathcal{G}^F$ where $\mathcal{G}^S$ is defined in terms of distribution of Rankine singularities, and $\mathcal{G}^F$ accounting for free-surface effects. Furthermore, $\mathcal{G}^F$ is decomposed, in [2] and [3], into a nonoscillatory local component $\mathcal{G}^N$ and a wave component $\mathcal{G}^W$ which is defined by the single Fourier integral

$$4\pi i\mathcal{G}^W=\int_{D=0}[(\Sigma_1+\Sigma_2)Se^{zk}/\|\nabla D\|]e^{-ih\varphi}\,ds \quad \text{with} \quad \varphi=\bar{x}\alpha+\bar{y}\beta,\ h=\sqrt{x^2+y^2},\ (\bar{x},\bar{y})=(x,y)/h \qquad (1)$$

along every dispersion curve defined in the Fourier plane (α,β) by the dispersion relation $D=0$. Here, ds is the arc length along a dispersion curve and $\|\nabla D\|^2=D_\alpha^2+D_\beta^2$. The function $\Sigma_1=\text{sign}(D_f)$ associated with the fact to satisfy the radiation condition is obtained by a formal analysis performed in [2], while Σ_2 is expressed in different ways in [3] according to the shape of the dispersion curve. The spectrum function $S(\alpha,\beta)$ is defined in terms of distribution of elementary waves over the mean wetted hull and the mean waterline of the ship. For the sake of simplicity, we consider here the special case of $S=1$ which corresponds to a source at the point (a,b,c), and $(x,y,z)=(\xi-a,\eta-b,\zeta+c)$, the expression (1) represents exactly the wave component of usual free-surface Green functions. Furthermore, the identity $\Sigma_2=\text{sign}(\bar{x}D_\alpha+\bar{y}D_\beta)$ given originally in [2] is used without loss of generality, since the extension to any form of Σ_2 and the spectral function S is straightforward.

The dispersion relation $D=0$ defines usually several dispersion curves. Each dispersion curve is related to a wave system. Wave systems can further be regrouped into different classes according to the type of associated dispersion curves. Analytical expressions of different classes of unsteady ship waves can be obtained by an asymptotical analysis of (1) and summarized hereafter.

2 Unsteady ship wave patterns

For the free-surface time-harmonic ship flows in deep water, the dispersion function $D(\alpha,\beta)$ is given by

$$D=(F\alpha-f)^2-k \quad \text{with} \quad k=\sqrt{\alpha^2+\beta^2} \qquad (2)$$

where $f=\omega\sqrt{L/g}$ and $F=U/\sqrt{gL}$ are respectively called nondimensional frequency and Froude number, as ω and U stand respectively for wave encounter frequency and ship's speed, and L and g for ship's length and the acceleration of gravity. The dispersion function (2) shows that the dispersion curves $D=0$ are symmetric with respect to $\beta=0$ and there exist three or two dispersion curves if $\tau=fF=\omega U/g$ is smaller or larger than $1/4$, respectively. For $\tau<1/4$, the three dispersion curves intersect the axis $\beta=0$ at four values of α, which are denoted $\alpha_i^\pm$ and $\alpha_o^\pm$ and given by

$$F^2\alpha_i^\pm=\tau\pm(1/2-\sqrt{1/4\pm\tau}) \quad \text{and} \quad F^2\alpha_o^\pm=\tau\pm(1/2+\sqrt{1/4\pm\tau}) \qquad (3)$$

such that two open dispersion curves are located in the regions $-\infty<\alpha\le\alpha_o^-$ and $\alpha_o^+\le\alpha<\infty$, and a close dispersion curve in the region $\alpha_i^-\le\alpha\le\alpha_i^+$. For $\tau>1/4$, we have only two open dispersion curves located in the regions $-\infty<\alpha\le\alpha_i^+$ and $\alpha_o^+\le\alpha<\infty$. In summary, there are two types of dispersion curves : a close dispersion curve for $\tau<1/4$ and two open dispersion curves for $F>0$. Analytical expressions of ship wave patterns associated with these two types of distinct dispersion curve are given now.

Ring waves - Close dispersion curve

The ring waves are associated with the close dispersion curve comprised between α_i^- and α_i^+ for $\tau<1/4$. The dispersion curve is described by a parametric equation

$$\alpha=k(\theta)\cos\theta,\quad \beta=k(\theta)\sin\theta \quad \text{with} \quad k^{1/2}=(\sqrt{1/4+\tau\cos\theta}-1/2)/(\tau\cos\theta) \qquad (4)$$

in which the variables (α,β,k) are understood to be multiplied by the frequency-scale factor $1/f^2$. The stationary point $(\alpha_r,\beta_r)=k_r(\cos\theta_r,\sin\theta_r)$ satisfying $\varphi'=0$ is determined by

$$\bar{x}\beta_r-\bar{y}(\alpha_r+2k_r^{3/2})=0 \quad \text{and} \quad \bar{y}\beta_r+\bar{x}(\alpha_r+2k_r^{3/2})<0 \tag{5a}$$

At the stationary point $\theta=\theta_r$, we define

$$\varphi_0^r=\bar{x}\alpha_r+\bar{y}\beta_r, \quad \varphi_2^r=\varphi_0^r[k_r''/k_r-2(k_r'/k_r)^2-1]/2, \quad \varphi_3^r=\varphi_0^r[(k_r'''-3k_r'k_r''/k_r-2k_r')/(3k_r)] \tag{5b}$$

where $k'=dk/d\theta$, $k''=d^2k/d\theta^2$ and $k'''=d^3k/d\theta^3$ are used. The analytical expression obtained from asymptotic analysis for the ring waves is written as

$$\mathcal{G}^R=\exp(-ih\varphi_0^r)A_0^r/\sqrt{(\varphi_3^r/\varphi_2^r)^4+ih\varphi_2^r} \quad \text{with} \quad A_0^r/f^2=-\frac{1}{4}ik_re^{zk_r}/\sqrt{\pi(1/4+\tau\cos\theta_r)} \tag{6}$$

which is of order $O(e^{-ih\varphi_0^r}/\sqrt{h})$ for $h\to\infty$ consistent with the classical result obtained from the stationary phase method. The fact that the analytical expression (6) has finite values at $h\to 0$ is expected so that it is well suited for numerical evaluations in the near field.

Transverse and divergent waves - Open dispersion curves

Three wave systems associated with open dispersion curves as defined in [3] are the inner-V waves corresponding to the right one located in $\alpha_o^+\le\alpha<\infty$ for $\tau>0$, the outer-V waves related to left open dispersion curve located in $-\infty<\alpha\le\alpha_o^-$ for $\tau<1/4$ and the ring-fan waves associated with left open dispersion curve located in $-\infty<\alpha\le\alpha_i^+$ for $\tau>1/4$. All open dispersion curves can be described by a unique parameter equation as

$$\alpha(u)=\tau-\Sigma_1\sqrt{k}, \quad \beta(u)=\sqrt{k^2-\alpha^2} \quad \text{with} \quad k=k_0(1+u^2) \tag{7}$$

for $0\le u<\infty$, in which the Fourier variables (α,β,k) are understood to be multiplied by the Froude-scale factor F^2. Furthermore, $\Sigma_1=-1$ and $k_0=F^2\alpha_o^+$ for the inner-V waves, $\Sigma_1=1$ for both outer-V and ring-fan waves while $k_0=-F^2\alpha_o^-$ for the outer-V waves and $k_0=F^2\alpha_i^+$ for the ring-fan waves.

The open dispersion curve described by (7) has an inflection point at $u=u_c$ determined by

$$k_c^2-(3/2)k_c+\Sigma_1 4\tau\sqrt{k_c}-3\tau^2=0 \tag{8a}$$

with $k_c=k(u_c)$ which gives the cusp angle with respect to the track of the source point

$$\gamma_c=\arctan(1/\sqrt{6k_c-1}) \tag{8b}$$

for both inner-V and outer-V waves, and for the ring-fan waves at $\tau>\sqrt{2/27}$ and

$$\gamma_c=\pi-\arctan(1/\sqrt{6k_c-1}) \tag{8c}$$

for the ring-fan waves in $1/4<\tau\le\sqrt{2/27}$. In fact, $\gamma_c=\pi/2$ at $\tau=\sqrt{2/27}$, i.e. strictly no waves propagate upstream for $\tau\ge\sqrt{2/27}$, an interesting exact result found in [5].

Following the analysis given in [1], there exist two points of stationary phase for $\gamma=\arctan[\bar{y}/(-\bar{x})]<\gamma_c$ at $u=u_t$ located in $[0,u_c]$ and $u=u_d$ in $[u_c,\infty)$ which are determined by

$$\bar{x}\beta_{t,d}-\bar{y}(\alpha_{t,d}+\Sigma_1 2k_{t,d}^{3/2})=0 \quad \text{and} \quad \operatorname{sign}[\bar{y}\beta_{t,d}+\bar{x}(\alpha_{t,d}+\Sigma_1 2k_{t,d}^{3/2})]=-\Sigma_1 \tag{9a}$$

with $(\alpha_{t,d},\beta_{t,d},k_{t,d})=[\alpha(u_{t,d}),\beta(u_{t,d}),k(u_{t,d})]$. At the stationary points $u=u_{t,d}$, we define

$$\varphi_0^{t,d}=\bar{x}\alpha_{t,d}+\bar{y}\beta_{t,d}, \quad \varphi_2^{t,d}=(\bar{x}\alpha_{t,d}''+\bar{y}\beta_{t,d}'')/2, \quad \varphi_3^{t,d}=(\bar{x}\alpha_{t,d}'''+\bar{y}\beta_{t,d}''')/3 \tag{9b}$$

where $(\alpha'',\beta'')=(d^2\alpha/du^2,d^2\beta/du^2)$ and $(\alpha''',\beta''')=(d^3\alpha/du^3,d^3\beta/du^3)$ are used. Corresponding to the stationary points (α_t,β_t,k_t) and (α_d,β_d,k_d), we may define respectively the transverse waves $\mathcal{G}^T$ and divergent waves $\mathcal{G}^D$. The analytical expressions for both transverse and divergent waves are written as

$$\mathcal{G}^T=\exp(-ih\varphi_0^t)\left(\frac{A_0^t\sqrt{\pi}}{\sqrt{(\varphi_3^t/\varphi_2^t)^4+ih\varphi_2^t}}+\frac{2}{3}\frac{A_0^t|\varphi_2^t/\varphi_3^t|}{(\sigma-ih\varphi_3^t/2)^{\frac{1}{6}}}\mathrm{K}_{\frac{1}{3}}\left[2(\sigma-ih\varphi_3^t/2)^{\frac{1}{2}}|\varphi_2^t/\varphi_3^t|^3\right]\right) \tag{10a}$$

$$\mathcal{G}^D=\exp(-ih\varphi_0^d)\left(\frac{A_0^d\sqrt{\pi}}{\sqrt{(\varphi_3^d/\varphi_2^d)^4+ih\varphi_2^d}}+\frac{2}{3}\frac{A_0^d|\varphi_2^d/\varphi_3^d|}{(\sigma+ih\varphi_3^d/2)^{\frac{1}{6}}}\mathrm{K}_{\frac{1}{3}}\left[2(\sigma+ih\varphi_3^d/2)^{\frac{1}{2}}|\varphi_2^d/\varphi_3^d|^3\right]\right) \tag{10b}$$

where $\mathrm{K}_{1/3}(w)$ is the modified Bessel function defined in [4] and σ a positive real constant. For $\gamma>\gamma_c$, we may use the values of (α_c,β_c,k_c) at the inflection point $u=u_c$ to define

$$\varphi_0^c=\bar{x}\alpha_c+\bar{y}\beta_c+\frac{(\bar{x}\alpha_c''+\bar{y}\beta_c'')^3}{3(\bar{x}\alpha_c'''+\bar{y}\beta_c''')^2}-\frac{(\bar{x}\alpha_c'+\bar{y}\beta_c')(\bar{x}\alpha_c''+\bar{y}\beta_c'')}{\bar{x}\alpha_c'''+\bar{y}\beta_c'''} \tag{11a}$$

$$\varphi_1^c=\bar{x}\alpha_c'+\bar{y}\beta_c'-\frac{1}{2}(\bar{x}\alpha_c''+\bar{y}\beta_c'')^2/(\bar{x}\alpha_c'''+\bar{y}\beta_c''') \quad \text{and} \quad \varphi_3^c=(\bar{x}\alpha_c'''+\bar{y}\beta_c''')/3 \tag{11b}$$

and the transverse and divergent waves by

$$\mathcal{G}^T = \exp(-ih\varphi_0^c)\left(\frac{A_0^c e^{-(h\varphi_1^c)^2(\varphi_1^c/\varphi_3^c)^4}}{2(\varphi_3^c/\varphi_1^c)^2} + \frac{2}{3}\frac{A_0^c|\varphi_1^c/\varphi_3^c|}{(\sigma - ih\varphi_3^c/2)^{\frac{1}{6}}}\,\mathrm{K}_{\frac{1}{3}}\Big[2(\sigma - ih\varphi_3^c/2)^{\frac{1}{2}}|\varphi_1^c/\varphi_3^c|^3\Big]\right) \tag{12a}$$

$$\mathcal{G}^D = \exp(-ih\varphi_0^c)\left(\frac{A_0^c e^{-(h\varphi_1^c)^2(\varphi_1^c/\varphi_3^c)^4}}{2(\varphi_3^c/\varphi_1^c)^2} + \frac{2}{3}\frac{A_0^c|\varphi_1^c/\varphi_3^c|}{(\sigma + ih\varphi_3^c/2)^{\frac{1}{6}}}\,\mathrm{K}_{\frac{1}{3}}\Big[2(\sigma + ih\varphi_3^c/2)^{\frac{1}{2}}|\varphi_1^c/\varphi_3^c|^3\Big]\right) \tag{12b}$$

The amplitude function $A_0^{t,d,c}$ involved in (10a), (10b), (12a) and (12b) are determined by

$$2\pi F^2 A_0^{t,d,c} = -\Sigma_1 ie^{zk_{t,d,c}}(\sqrt{k_0 k_{t,d,c}}/\beta_{t,d,c})\sqrt{k_{t,d,c} - k_0} \tag{13}$$

It can be checked that the second term in both (10a) for $\mathcal{G}^T$ and (10b) for $\mathcal{G}^D$, involving $\mathrm{K}_{1/3}$ decreases exponentially for $h \to \infty$ as far as $\varphi_2^{t,d} \neq 0$ and that both transverse and divergent waves decrease at a rate of order $O(h^{-1/2})$ within the wedge $\gamma < \gamma_c$. Along the wedge $\gamma = \gamma_c$, it can be shown that (10a) and (10b) are of order $O(h^{-1/3})$ as $\varphi_c^{t,d} \to 0$, consistent with the classical results. The amplitude of $\mathcal{G}^T$ represented by (12a) and $\mathcal{G}^D$ by (12b) decreases exponentially for $\varphi_1^c \neq 0$, i.e. $\gamma > \gamma_c$, and at a rate of order $O(h^{-1/3})$ when $\varphi_1^c \to 0$, i.e. $\gamma \to \gamma_c$, and equal to the results by (10a) and (10b).

3 Discussions and conclusions

We have summarized in this study analytical expressions of four ship-wave systems each of which is associated with a distinct dispersion curve by regrouping them into three classes. The first associated with a closed dispersion curve is called ring waves. The second associated with the portion of open dispersion curves limited between two inflexion points located symmetrically in the upper and lower half Fourier plane, is called transverse waves. The third class of unsteady ship waves is associated with the portions of open dispersion curves from the inflexion points to infinity, and called divergent waves. The ring waves propagate out in all directions for limited values of the Brard number $\tau < 1/4$ and their amplitude decreases at a rate of order $O(h^{-\frac{1}{2}})$ at $h \to \infty$. The transverse and divergent waves are limited by a cusp line whose angle defined by (8b) and (8c) is parallel to the direction of the normal vector at the inflection of corresponding dispersion curve. Within the wedge limited by the cusp line, the amplitude of transverse and divergent waves decreases at the same rate like $O(h^{-\frac{1}{2}})$ while along the wedge the decreasing rate is of $O(h^{-\frac{1}{3}})$. Outside the wedge, the non-oscillatory local component is dominant since the decreasing rate is of order $O(h^{-1})$ while the wave amplitude falls off exponentially. These important features of transverse and divergent waves are well described by (10a) and (10b) within the wedge, (12a) and (12b) outside the wedge. Furthermore, the expressions (10a) and (12a) for transverse waves as well as (10b) and (12b) for divergent waves provide the same and correct asymptotic values along the wedge so that they are continuous across the wedge, as shown by Fig.1 and Fig.2 which depict $\mathcal{G}^T + \mathcal{G}^D$ of the inner-V waves at $\tau = 1/4$. In both figures, the real and imaginary parts of $\mathcal{G}^T + \mathcal{G}^D$ are presented by the solid and dashed lines, respectively. The value $z = 0$ is used on Fig.1 and $z/F^2 = -0.1$ on Fig.2.

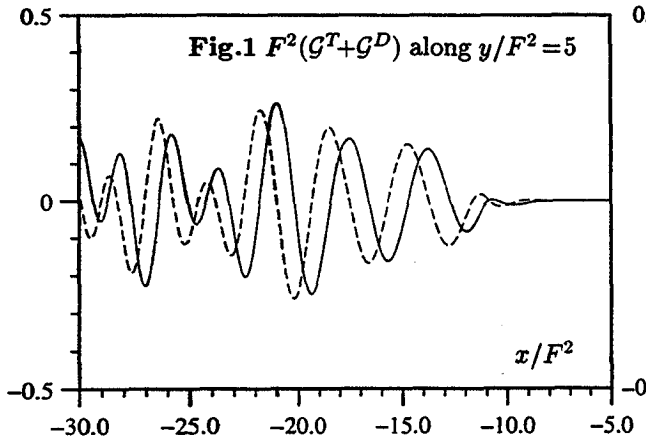

Fig.1 $F^2(\mathcal{G}^T + \mathcal{G}^D)$ along $y/F^2 = 5$

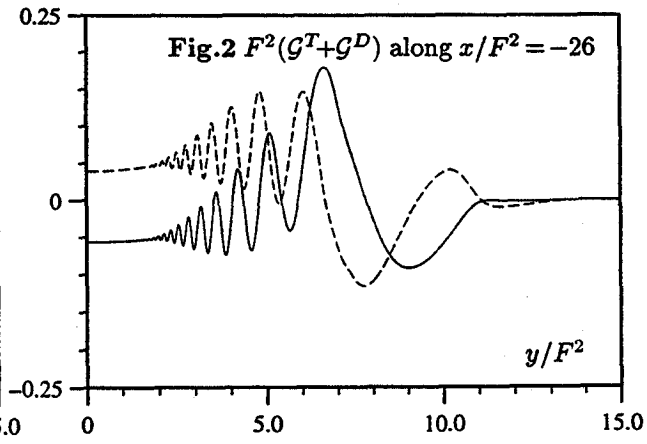

Fig.2 $F^2(\mathcal{G}^T + \mathcal{G}^D)$ along $x/F^2 = -26$

The classical treatments to the phase function which exhibits two coalescing stationary points were presented in [6] to develop uniform asymptotic expansions of an integral. Very fine results can be obtained as presented in [7] in applying to the Neumann-Kelvin steady waves. However, we prefer here forgoing expressions obtained in a different way (which will be presented elsewhere for the sake of space) to describe more complicated *unsteady* ship waves for several reasons.

Firstly, the expressions (10a) for transverse waves $\mathcal{G}^T$ and (10b) for divergent waves $\mathcal{G}^D$ are *explicit* in that the wavenumbers $k^{t,d}$, more exactly wavenumber vectors $(\alpha_{t,d}, \beta_{t,d})$, corresponding to the stationary points

$k_0 \le k_t < k_c$ and $k_c < k_d < \infty$ partitioned by k_c given at the inflection point of the corresponding dispersion curve. The decreasing rate is of order $(h^{-1/2})$ since the terms involving $K_{1/3}$ are exponentially small at $h \to \infty$ for a given $\gamma < \gamma_c$. At the wedge $\gamma = \gamma_c$, we have $k_t = k_c = k_d$ and the terms involving $K_{1/3}$ are reduced to those of order $O(h^{-1/3})$ while the first terms in (10a) and (10b) tend to zero as $\varphi_2^{t,d} \to 0$. The transverse waves $\mathcal{G}^T$ and the divergent waves $\mathcal{G}^D$ involved in the inner-V waves, are depicted separately on Fig.3 at $\tau = 1/4$, $z/F^2 = -0.01$ and $\gamma = \gamma_c/2$ with $\tan(\gamma_c) = \sqrt{2/25}$. Fig.4 shows the sum $\mathcal{G}^T + \mathcal{G}^D$ and compared with the line integral (1). It is shown that the difference between analytical expressions (10a) and (10b) and the line integral (1), represented by the thick solid and dashed lines, is negligible for $F^2 h > 10$. In both Fig.3 and Fig.4, the solid and dashed lines represent the real and imaginary parts, respectively.

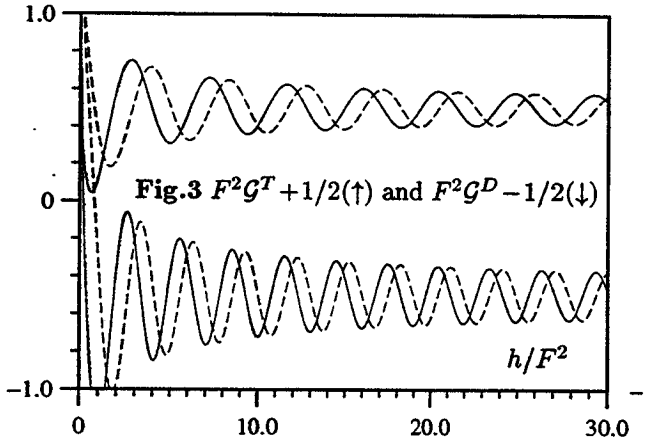

Fig.3 $F^2\mathcal{G}^T + 1/2(\uparrow)$ and $F^2\mathcal{G}^D - 1/2(\downarrow)$

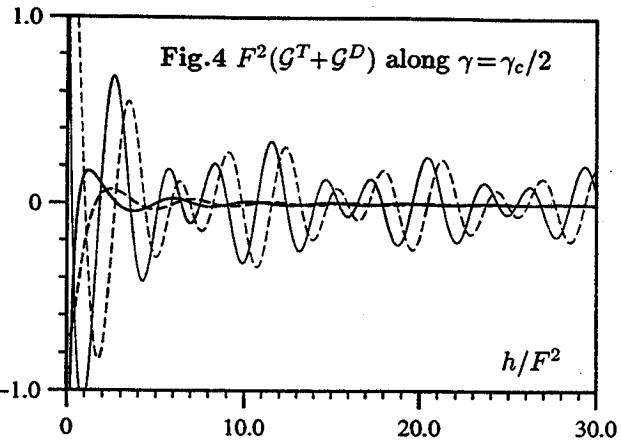

Fig.4 $F^2(\mathcal{G}^T + \mathcal{G}^D)$ along $\gamma = \gamma_c/2$

Concerning divergent waves defined by (10b), as already noted, the decreasing rate is of $O(h^{-\frac{1}{2}})$ in a given direction within the wedge and $O(h^{-\frac{1}{3}})$ along the wedge as well as the transverse waves. However, for a field point in the downstream $\bar{x} < 0$ with $\bar{y} \to 0$, the values of the stationary point (α_d, β_d, k_d) defined by (9a) are given approximately

$$\alpha_d \sim -\Sigma_1 \bar{x}/(2\bar{y}), \quad \beta_d \sim \bar{x}^2/(4\bar{y}^2) \quad \text{and} \quad k_d \sim \bar{x}^2/(4\bar{y}^2) \tag{14}$$

as the leading term. The amplitude function A_0^d defined by (13) decreases exponentially for a field point approaching to the track of an *immerged* source point ($z < 0$). Furthermore, if $z = 0$ and $\bar{y} \to 0$, i.e. a field point approaches to the track of a source located *at* the free surface, the divergent waves are highly oscillatory with infinitely increasing amplitude and infinitely decreasing wavelength, since $\varphi_2^d \sim k_0 \bar{y}$ and $\varphi_3^d/\varphi_2^d \sim 0$ involved in (10b). This singular and highly-oscillatory properties of ship waves are analyzed in [8] in great detail.

Secondly, the expressions (6) for ring waves, (10a) and (12a) for transverse waves, and (10b) and (12b) for divergent waves are *regular* in the near field even for $h \to 0$, which is not the case in classical asymptotic analysis. Far-field waves represented by these analytical expressions are extended to the near field and complementary to the local component which is dominant. Finally, the last but not the least concerns calculating the line integral (1) in a complete way. Indeed, the asymptotic analysis performed to obtain the analytical expressions, provides formulations well suited for numerical evaluations of the remaining term - another line integral with the integrand of (1) after subtracting the terms related to the analytical expressions.

In summary, we have given the new expressions of unsteady ship wave patterns in an analytical form. These expressions are critically important in calculating the ship-motion Green function in the far field. They may be very useful as well in a number of analyzes such as estimating wave-damping and wave-resistance components.

References

[1] CHEN X.B. & NOBLESSE F. 1997 Dispersion relation and far-field waves. *12th IWWWFB.*

[2] NOBLESSE F. & CHEN X.B. 1995 Decomposition of free-surface effects into wave and near-field components. *Ship Technology Research* Vol.42, 167-185.

[3] CHEN X.B. & NOBLESSE F. 1998 Super Green Functions. *22nd Symposium on Naval Hydrodynamics.*

[4] ABRAMOWITZ M. & STEGUN I.A. 1967 Handbook of mathematical functions. *Dover Publications.*

[5] CHEN X.B. 1996 Evaluation des champs de vagues générés par un navire avançant dans la houle, *Rapport final du Projet DRET/BV* no.95 378.

[6] CHESTER C., FRIEDMAN & URSELL F. 1956 An extension of the method of steepest descents, *Proc. Camb. Phil. Soc.* Vol.53, 599-611.

[7] URSELL F. 1960 On Kelvin's ship-wave pattern. *J. Fluid Mech.* vol.8, 418-431.

[8] CHEN X.B. 1998 On singular and highly-oscillatory properties of the ship-motion Green function. *Submitted for publication.*